magnetochemistry

MDPI

Communication

In Situ Tuning of Magnetism in Fe_3GeTe_2 via Argon Ions Irradiation

Shan Wang [1], Chuanwu Cao [1] and Jian-Hao Chen [1,2,3,4,*]

[1] International Center for Quantum Materials, School of Physics, Peking University, Beijing 100871, China
[2] Beijing Academy of Quantum Information Sciences, Beijing 100193, China
[3] Key Laboratory for the Physics and Chemistry of Nanodevices, Peking University, Beijing 100871, China
[4] Hefei National Laboratory, Hefei 230088, China
* Correspondence: chenjianhao@pku.edu.cn

Abstract: We report the continuous argon ions irradiation of itinerant Fe_3GeTe_2, a two-dimensional ferromagnetic metal, with the modification to its transport properties measured *in situ*. Our results show that defects generated by argon ions irradiation can significantly weaken the magnetization (M) and coercive field (H_c) of Fe_3GeTe_2, demonstrating the tunable magnetism of this material. Specifically, at base temperature, we observed a reduction of M and H_c by up to 40% and 62.4%, respectively. After separating the contribution from different mechanisms based on the Tian-Ye-Jin (TYJ) scaling relation, it's the skew scattering that dominates the contribution to anomalous Hall effect in argon ions irradiated Fe_3GeTe_2. These findings highlight the potential of *in situ* transport modification as an effective method for tailoring the magnetic properties of two-dimensional magnetic materials, and provides new insights into the mechanisms underlying the tunable magnetism in Fe_3GeTe_2.

Keywords: two-dimensional magnetism; *in situ* transport; Fe_3GeTe_2

Citation: Wang, S.; Cao, C.; Chen, J.-H. *In Situ* Tuning of Magnetism in Fe_3GeTe_2 via Argon Ions Irradiation. *Magnetochemistry* **2023**, *9*, 125. https://doi.org/10.3390/magnetochemistry9050125

Academic Editor: Bo Li

Received: 5 April 2023
Revised: 29 April 2023
Accepted: 4 May 2023
Published: 9 May 2023

1. Introduction

The field of two-dimensional (2D) layered materials has experienced rapid growth since the discovery of graphene in 2004 [1–9]. Significant research efforts have been devoted to studying the electrical, optical, and topological properties of 2D materials, with notable achievements in phenomena such as the quantum Hall effect (QHE) [4], valley Hall effect (VHE) [10] and nonlinear Hall effect (NLHE) [11–13]. However, the discovery and study of 2D layered magnetic materials has been surprisingly delayed until 2017, when the confirmation of the existence of long-range magnetic order is achieved by magnetic crystalline anisotropy in single-layer CrI_3 [14] and by the application of a small external magnetic field in $Cr_2Ge_2Te_6$ [15]. As a result, much attention has been devoted to the search for and tuning of 2D magnets with higher Curie temperatures (T_c) in order to further explore their mechanisms and potential applications [16–21]. Recent advancements, such as the ionic-gate tunable room temperature 2D itinerant magnet in Fe_3GeTe_2, using an Al_2O_3 assisted exfoliation method [22], have inspired various modulation techniques including gate-controlled Li^+ doping and Fe defects [22–24]. However, despite these developments, understanding the modulation of magnetic properties, particularly the anomalous Hall effect, remains an active area of research and requires further investigation.

With its high surface-to-volume ratio, thin layered materials possess excellent surface sensitivity and can be effectively modified by surface treatments such as doping, irradiation and etching [25–28]. *In situ* modification measurements can ensure that the physical properties are only affected by the intended modifications and exclude unwanted influences, thereby improving the accuracy of tuning particularly sensitive materials. *In situ* transport measurements have demonstrated unique advantages in materials such as Co-decorated graphene [29], hydrogenated graphene [30] and so on [31,32]. Therefore, combining tunable

thin flake Fe_3GeTe_2 with *in situ* transport provides an exciting opportunity to explore the mechanism of anomalous Hall effect and the tuning of magnetic properties.

In this study, we report on the tunable magnetic properties of argon ions irradiated thin flake Fe_3GeTe_2, where the remanent Hall resistance (R^r_{xy}) and coercive field (H_c) decreased with increasing irradiation. The anomalous Hall effect in irradiated Fe_3GeTe_2 mainly originates from skew scattering induced by argon ions by scaling analysis. Our results suggest that argon irradiation can effectively tune the magnetic properties of Fe_3GeTe_2 and provide valuable insights into the underlying physics of this system.

2. Materials and Methods

In this work, we report the tunable magnetic properties of argon-irradiated thin flakes of Fe_3GeTe_2. The exfoliation of thin flakes of Fe_3GeTe_2 on SiO_2/Si substrates was assisted by the evaporation of Al_2O_3, as previously described [22]. Cr/Au (3 nm/70 nm) electrodes were evaporated onto the thin flakes of Fe_3GeTe_2 through stencil masks to avoid any possible degradation from the conventional lithography process. The fabrication process was conducted in a glovebox to preserve sample quality. Seven runs of argon ions irradiation were performed, and the transport properties of Fe_3GeTe_2 were studied *in situ* after each round using the lock-in detection technique. The simplified schematic of the *in situ* transport measurement setup is shown in Figure 1a, and the base temperature was maintained at 10 K. The argon ions generation was accomplished through a radio-frequency ions source with a working voltage of 2 kV and current of 20 mA. The irradiation time was in the range of 5–10 s for each run.

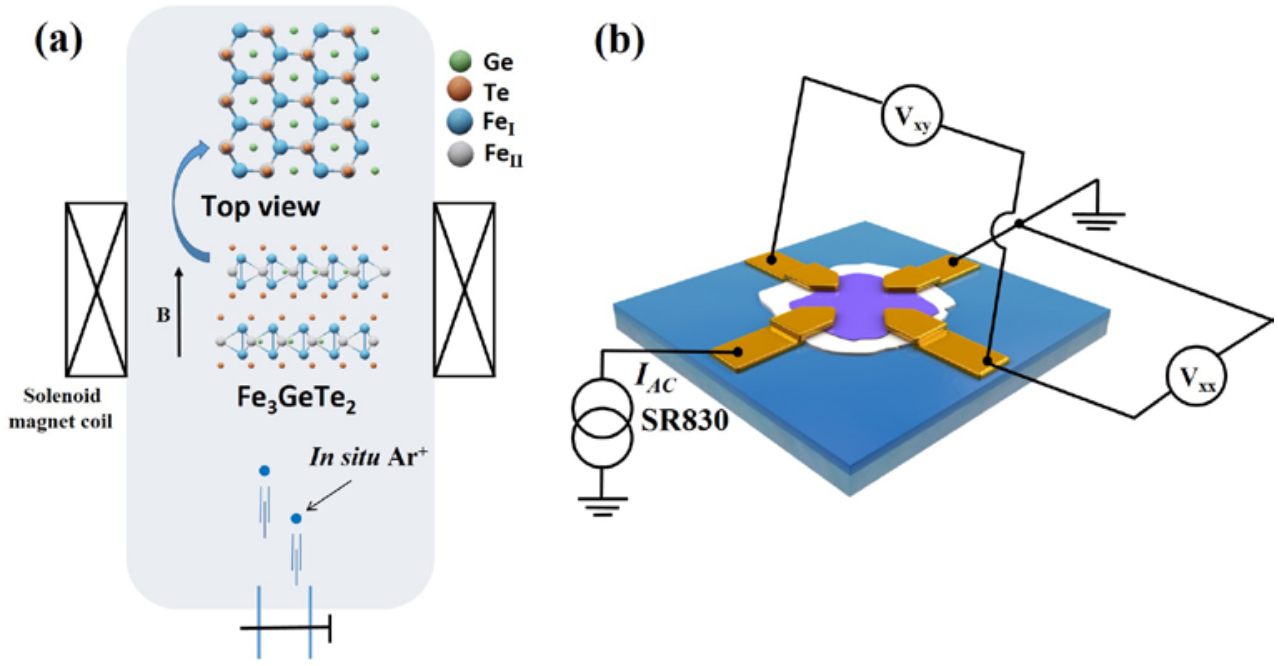

Figure 1. The simplified schematic of *in situ* transport measurement setup for argon ions irradiated thin flake Fe_3GeTe_2 device. (**a**)The demonstration of *in situ* irradiation process, the gray area in the center represents vacuum environment. (**b**)The electrical measurement geometry of thin flake Fe_3GeTe_2 device on SiO_2/Si substrate.

3. Results

In ferromagnetic (FM) materials, the transverse Hall resistance comprises ordinary Hall and anomalous Hall terms, which can be expressed as a function of the applied magnetic field and magnetization [33]:

$$R_{xy} = R_0 \mu_0 H + R_S M \quad (1)$$

where R_0 and R_S represent the ordinary Hall coefficient and anomalous Hall coefficient, respectively; H is the applied magnetic field perpendicular to the sample surface and M is the magnetization. The R_{xy} under zero magnetic field after the application of saturation magnetic field is called the remanent Hall resistance (R^r_{xy}), which is proportional to the spontaneous magnetization and reflects the long-range FM order of the sample. In this study, we investigated the magnetic properties of thin flake Fe_3GeTe_2 through transport measurements. The temperature-dependent Hall resistance (R_{xy}) of the pristine sample as a function of applied magnetic field is shown in Figure 2a, revealing square-shaped magnetic hysteresis below 140 K, indicating the presence of a single magnetization domain and confirming the establishment of long-range FM order in the sample. As shown in Figure 2b, the R^r_{xy} of the pristine sample appears at 140 K and increases to 3.45 Ω at 10 K. Since R^r_{xy} is proportional to the zero field spontaneous magnetization, the onset of non-zero R^r_{xy} represents the appearance of long-range magnetic order below 140 K, which indicates that the Curie temperature is around 140 K. Thus determining the thickness of our sample to be approximately 3.2 nm (four layers) according to previous transport reports [22]. The coercive field (H_c) increases from 0.0076 T at 120 K to 0.1255 T at 10 K; at higher temperatures the hysteresis loop disappears due to thermal fluctuations.

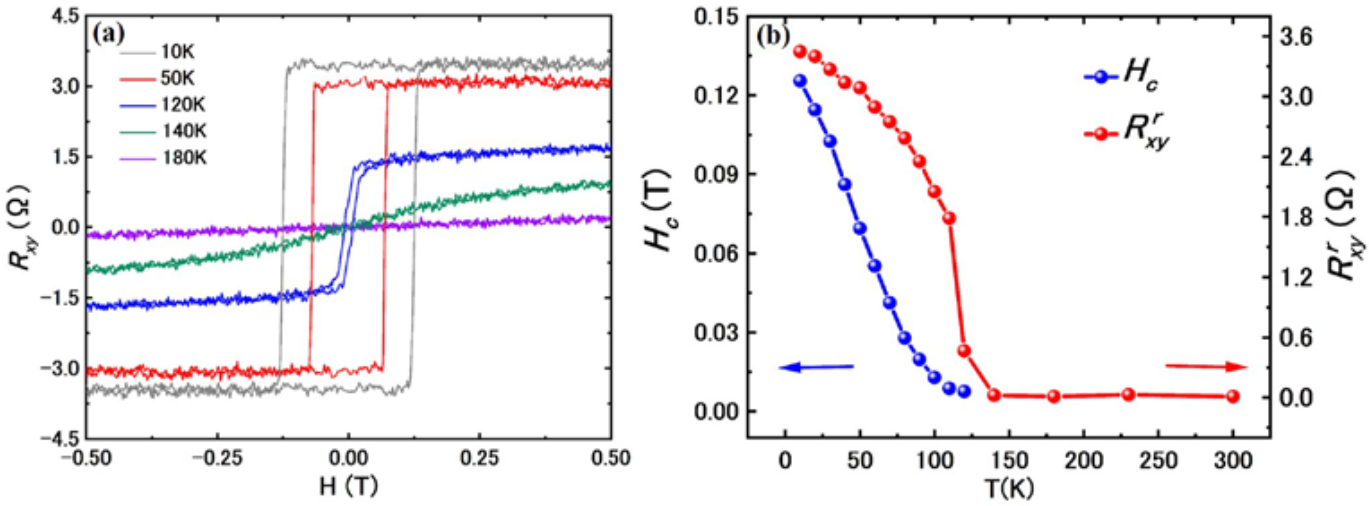

Figure 2. The characterization of magnetic properties by transport in pristine thin flake Fe_3GeTe_2. (**a**) Hall resistance (R_{xy}) as a function of magnetic field (perpendicular to plane) at 10–180 K. (**b**) Remanent Hall resistance (R^r_{xy}) and coercive field (H_c) vs. T.

In order to explore the irradiation tunability of thin flakes Fe_3GeTe_2, we conducted *in situ* irradiation with argon ions and transport measurement. As depicted in Figure 3a, R^r_{xy} for each run of irradiation shows similar behavior with temperature, but the overall curves are decreasing with increasing Ar^+ irradiation under the same temperature. At base temperature, the R^r_{xy} of the pristine sample was measured to be 3.45 Ω, while after the seventh irradiation, it decreased to 2.08 Ω. This indicates a ~40% reduction in magnetization, as shown in Figure 3b, which suggests that the magnetization is disrupted by defects induced by argon ions.

In recent reports, the "chemical pressure" generated by substituting Ni or Co into the Fe sites, played an important role in suppressing ferromagnetism in $Fe_{3-x}GeTe_2$ crystals [34–37]. They all showed a significant modification of Curie temperature accompanied by the change of lattice parameters. Taking Fe_3GeTe_2 substituted by non-magnetic nickel (Ni) as an example [36], the long-range FM order was smeared into a glassy phase and even vanished above the inflection point around x = 0.3 in $(Fe_{1-x}Ni_x)_3GeTe_2$ (x = 0–0.84). However, although the R^r_{xy} can be greatly tuned by Ar^+ irradiation in our report, the onset temperature with the appearance of R^r_{xy} accompanied by FM hysteresis is almost unchanged, which indicates that the long-range FM order always persists and was not

destroyed by defects. Therefore, the irradiated Fe_3GeTe_2 will provide a good platform for continuously controllable modification with persisting long-range FM order.

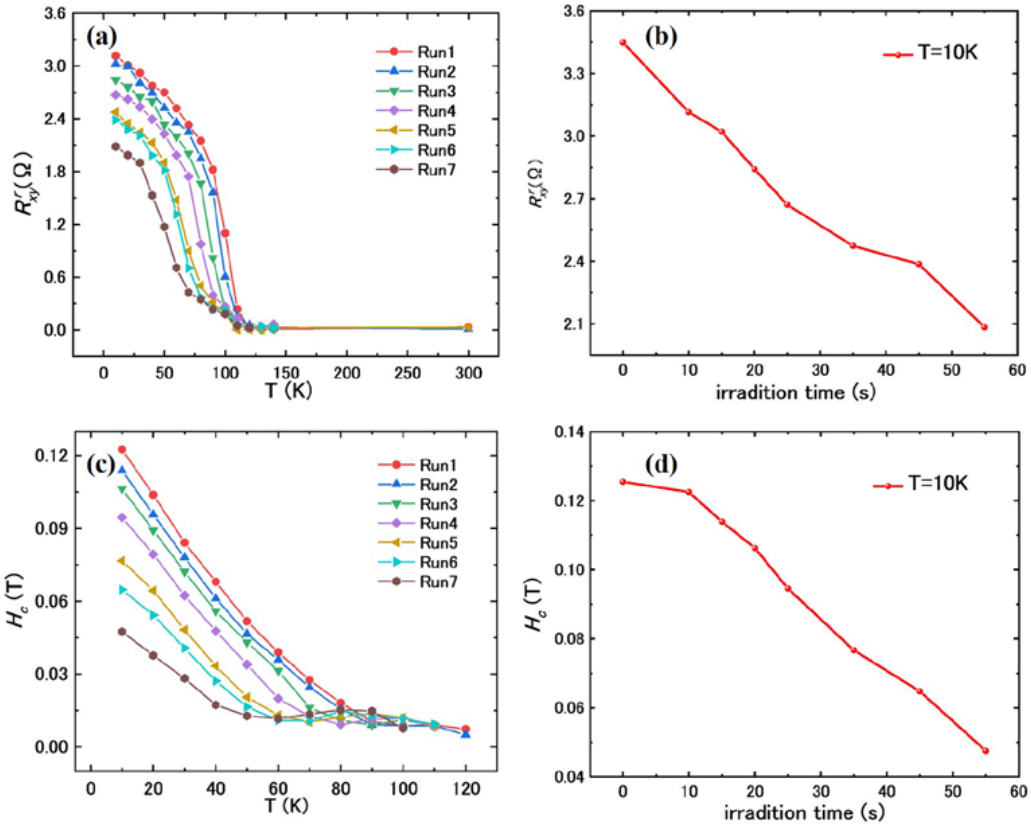

Figure 3. The change of remanent hall resistance (R_{xy}^r) and coercive field (H_c) in thin flake Fe_3GeTe_2 by argon ions irradiation. (**a**,**c**) R_{xy}^r and H_c vs. T after each round of argon doping. (**b**,**d**) R_{xy}^r and H_c after each round of argon ions irradiation at 10 K.

Apart from R_{xy}^r, the coercive field (H_c) is another crucial parameter for characterizing magnetic properties. We found that H_c can also be modified by the introduction of defects, as demonstrated in Figure 3c. It is worth noting that the H_c value drops by approximately 62.4% from 0.125 T to 0.047 T at 10 K after seven rounds of irradiation with argon ions, as depicted in Figure 3d. This finding suggests that defects induced by argon ions does not induce domain wall pinning, but rather, reduces such pinning in Fe_3GeTe_2, resulting in a reduction in the coercivity. Notably, the slight bump in H_c observed after the sixth round of irradiation at 60–90 K may stem from the local magnetic moment and warrants further investigation using other characterization techniques in future studies.

Combined with the report from previous neutron and X-ray diffraction studies about Fe-deficient $Fe_{3-x}GeTe_2$ [38], we can speculate that the suppressed magnetization in Ar^+ irradiated Fe_3GeTe_2 probably derived from increasing vacancies on the Fe(2) site generated by implanted argon ions, although the confirmation of which requires a scanning tunneling experiment in the future. The increasing disorder and magnetic dilution via vacancies may cause a disruption of the magnetic exchange and induce the suppressed magnetism. More efforts, such as theoretical simulation, adatoms doping, should be investigated in the future.

To summarize, our above results demonstrate that defects generated by argon ions irradiation can effectively tune the magnetization and coercivity of Fe_3GeTe_2 *in situ*, highlighting the potential of *in situ* transport measurement as a powerful tool for modifying the magnetic properties of materials.

4. Discussion

The scaling between anomalous Hall resistivity (ρ_{ah}) and longitudinal resistivity (ρ_{xx}) provided by Xiaofeng Jin et al. can clearly separate the contribution involving skew scattering, side jump and Berry curvature [39], which was widely used in the analysis of anomalous Hall effect [40]. This scaling is also called the TYJ scaling relation and can be expressed as:

$$\rho_{ah} = a'\rho_{xx0} + a''\rho_{xxT} + b\rho_{xx}^2 \quad (2)$$

where the ρ_{xx0} and ρ_{xxT} represent the residual resistivity at zero temperature and the phonon-induced resistivity at temperature T, respectively. They satisfy the relationship of $\rho_{xx} = \rho_{xx0} + \rho_{xxT}$. The parameters a' and a'' represent the impurity and phonon contribution to the skew scattering, and the parameter b represents joint contributions from the extrinsic side-jump and intrinsic Berry curvature.

To gain further insight into the reduction of magnetism in Ar^+ irradiated Fe_3GeTe_2, we employ fitting between ρ_{ah} and ρ_{xx} based on Equation (2) to determine contribution from different mechanisms. The longitudinal resistivity (ρ_{xx}) is obtained by the relation of $\rho_{xx} = \frac{R_{xx} \cdot d}{L/W}$, where the d is the thickness of device and the L/W is the aspect ratio between the measured electrodes. The transverse resistivity (ρ_{xy}) is derived according to the relation of $\rho_{xy} = R_{xy} \cdot d$. Wherein the $R_{xx}(R_{xy})$ is the longitudinal (transverse) resistance after the standard symmetrization (anti-symmetrization) procedure [22,33]. Then the anomalous Hall resistivity (ρ_{ah}) can be determined by extrapolating the high field (H > 1 T) part of ρ_{xy} back to zero field. The fitting results are shown in Figure 4 for data from the Ar^+ irradiation run 2–7, which demonstrated the applicability of the TYJ scaling relation.

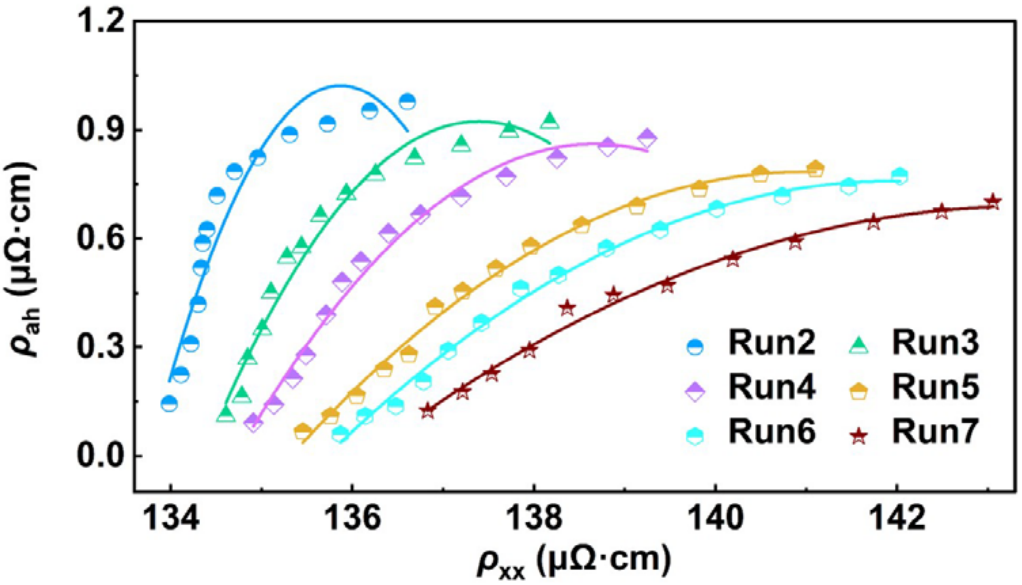

Figure 4. The fitting of ρ_{ah} and ρ_{xx} with Ar^+ irradiation run 2–7. The solid lines are fitting results with $\rho_{ah} = a'\rho_{xx0} + a''\rho_{xxT} + b\rho_{xx}^2$, and the colored symbols are experimental data.

Next, we plot the fitting parameters a', a'', and b with irradiation time as shown in Figure 5. First, it is obvious from the parameters that the skew scattering contribution dominates the anomalous Hall effect due to higher value. Moreover, the opposite sign between a' (a'') and b indicates that the contribution between joint contribution from intrinsic Berry curvature as well as side-jump and skew scattering is opposite, which was also observed recently in pristine single crystal Fe_3GeTe_2 [41]. As irradiation time increases, the amplitude of a',a'', and b gradually decrease, especially in the range of the first 15–25 s, then tend to zero. This means that the defects generated by Ar^+ irradiation can effectively reduce the skew scattering strength in Fe_3GeTe_2. Ar^+ irradiation can also strongly reduce the combined effect of Berry curvature and side-jump scattering in the material. The overall

effect is that the scattering in Ar^+ irradiated Fe_3GeTe_2 becomes increasingly non-magnetic, which is an interesting observation, since the contribution from magnetic scattering reduces drastically when disorders are introduced.

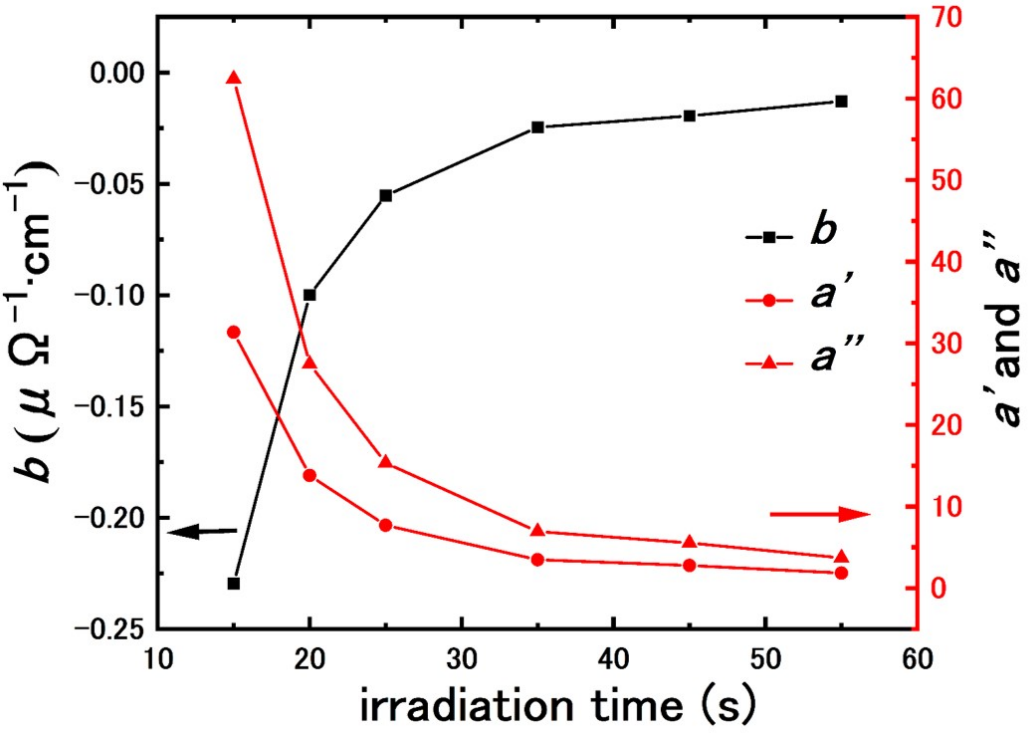

Figure 5. The circular, triangular, and square symbols represent the fitting parameters a', a'' and b to the TYJ scaling relation, respectively. The solid curves are guide to the eye.

5. Conclusions

In conclusion, we have demonstrated the tunable magnetism of Fe_3GeTe_2 via *in situ* argon ions irradiation and subsequent transport measurement in continuous vacuum environment. Our results show that defects induced by argon ions can significantly weaken the magnetization, with a 40% reduction observed at base temperature after seven runs of irradiation in 4 layers of Fe_3GeTe_2. Additionally, we observed a 62.4% decrease in the coercive field at 10K, meaning the magnetic domain wall pinning effect is also weakened by the disorder, contrary to common expectation [22,42]. The suppressed magnetization might stem from increasing vacancies generated by argon ions irradiation on the Fe(2) site in Fe_3GeTe_2. The persisting long-range FM order below onset temperature is different from chemical doping Fe_3GeTe_2, which showed vanished long-range FM order with doping. Moreover, the TYJ scaling reveals that the main contribution to the anomalous Hall effect is from skew scattering. The scaling shows that Ar^+ irradiation strongly reduces the effect of skew scattering, side-jump and Berry curvature, turning charge carriers scattering in Ar^+ irradiated Fe_3GeTe_2 to become increasingly non-magnetic. Finally, these show that magnetism in Fe_3GeTe_2 is highly tunable by disorders, and emphasize the powerful capability of *in situ* transport measurements to clarify the magnetic properties and scattering mechanisms of low-dimensional magnetic materials.

Author Contributions: Conceptualization, J.-H.C.; methodology, J.-H.C.; validation, S.W., C.C. and J.-H.C.; formal analysis, S.W. and C.C.; investigation, S.W. and C.C.; resources, J.-H.C.; data curation, S.W. and C.C.; writing—original draft preparation, S.W., C.C. and J.-H.C.; writing—review and editing, S.W., C.C. and J.-H.C.; visualization, S.W., C.C. and J.-H.C.; supervision, J.-H.C.; project administration, J.-H.C.; funding acquisition, J.-H.C. All authors have read and agreed to the published version of the manuscript.

Funding: This research was funded by the National Key R&D Program of China (Grant Nos. 2019YFA0308402, 2018YFA0305604), the Innovation Program for Quantum Science and Technology (2021ZD0302403), the National Natural Science Foundation of China (NSFC Grant Nos. 11934001, 92265106, 11774010, 11921005), Beijing Municipal Natural Science Foundation (Grant No. JQ20002).

Institutional Review Board Statement: Not applicable.

Informed Consent Statement: Not applicable.

Data Availability Statement: All data associated with this manuscript is published in the text.

Acknowledgments: We thank Xinjian Wei, Shaobo Liu, Yinan Liu, and Yinong Zhang for the helpful discussion. J.-H.C. acknowledge the technical supports from Peking Nanofab.

Conflicts of Interest: The authors declare no conflict of interest.

References

1. Novoselov, K.S.; Geim, A.K.; Morozov, S.V.; Jiang, D.; Zhang, Y.; Dubonos, S.V.; Grigorieva, I.V.; Firsov, A.A. Electric field effect in atomically thin carbon films. *Science* **2004**, *306*, 666–669. [CrossRef] [PubMed]
2. Novoselov, K.S.; Geim, A.K.; Morozov, S.V.; Jiang, D.; Katsnelson, M.I.; Grigorieva, I.V.; Dubonos, S.V.; Firsov, A.A. Two-dimensional gas of massless Dirac fermions in graphene. *Nature* **2005**, *438*, 197–200. [CrossRef] [PubMed]
3. Novoselov, K.S.; Jiang, D.; Schedin, F.; Booth, T.J.; Khotkevich, V.V.; Morozov, S.V.; Geim, A.K. Two-dimensional atomic crystals. *Proc. Natl. Acad. Sci. USA* **2005**, *102*, 10451–10453. [CrossRef] [PubMed]
4. Zhang, Y.; Tan, Y.-W.; Stormer, H.L.; Kim, P. Experimental observation of the quantum Hall effect and Berry's phase in graphene. *Nature* **2005**, *438*, 201–204. [CrossRef]
5. Ferrari, A.C.; Meyer, J.C.; Scardaci, V.; Casiraghi, C.; Lazzeri, M.; Mauri, F.; Piscanec, S.; Jiang, D.; Novoselov, K.S.; Roth, S.; et al. Raman spectrum of graphene and graphene layers. *Phys. Rev. Lett.* **2006**, *97*, 187401. [CrossRef]
6. Geim, A.K.; Novoselov, K.S. The rise of graphene. *Nat. Mater.* **2007**, *6*, 183–191. [CrossRef]
7. Balandin, A.A.; Ghosh, S.; Bao, W.; Calizo, I.; Teweldebrhan, D.; Miao, F.; Lau, C.N. Superior thermal conductivity of single-layer graphene. *Nano Lett.* **2008**, *8*, 902–907. [CrossRef]
8. Castro Neto, A.H.; Guinea, F.; Peres, N.M.R.; Novoselov, K.S.; Geim, A.K. The electronic properties of graphene. *Rev. Mod. Phys.* **2009**, *81*, 109–162. [CrossRef]
9. Novoselov, K.S.; Fal'ko, V.I.; Colombo, L.; Gellert, P.R.; Schwab, M.G.; Kim, K. A roadmap for graphene. *Nature* **2012**, *490*, 192–200. [CrossRef]
10. Mak, K.F.; McGill, K.L.; Park, J.; McEuen, P.L. The valley Hall effect in MoS_2 transistors. *Science* **2014**, *344*, 1489–1492. [CrossRef]
11. Ma, Q.; Xu, S.-Y.; Shen, H.; MacNeill, D.; Fatemi, V.; Chang, T.-R.; Mier Valdivia, A.M.; Wu, S.; Du, Z.; Hsu, C.-H.; et al. Observation of the nonlinear Hall effect under time-reversal-symmetric conditions. *Nature* **2019**, *565*, 337–342. [CrossRef]
12. Tiwari, A.; Chen, F.; Zhong, S.; Drueke, E.; Koo, J.; Kaczmarek, A.; Xiao, C.; Gao, J.; Luo, X.; Niu, Q.; et al. Giant c-axis nonlinear anomalous Hall effect in Td-$MoTe_2$ and WTe_2. *Nat. Commun.* **2021**, *12*, 2049. [CrossRef]
13. Huang, M.; Wu, Z.; Hu, J.; Cai, X.; Li, E.; An, L.; Feng, X.; Ye, Z.; Lin, N.; Law, K.T.; et al. Giant nonlinear Hall effect in twisted bilayer WSe_2. *Natl. Sci. Rev.* **2022**, nwac232. [CrossRef]
14. Huang, B.; Clark, G.; Navarro-Moratalla, E.; Klein, D.R.; Cheng, R.; Seyler, K.L.; Zhong, D.; Schmidgall, E.; McGuire, M.A.; Cobden, D.H.; et al. Layer-dependent ferromagnetism in a van der Waals crystal down to the monolayer limit. *Nature* **2017**, *546*, 270–273. [CrossRef]
15. Gong, C.; Li, L.; Li, Z.; Ji, H.; Stern, A.; Xia, Y.; Cao, T.; Bao, W.; Wang, C.; Wang, Y.; et al. Discovery of intrinsic ferromagnetism in two-dimensional van der Waals crystals. *Nature* **2017**, *546*, 265–269. [CrossRef]
16. Burch, K.S.; Mandrus, D.; Park, J.-G. Magnetism in two-dimensional van der Waals materials. *Nature* **2018**, *563*, 47–52. [CrossRef]
17. Jiang, S.; Li, L.; Wang, Z.; Mak, K.F.; Shan, J. Controlling magnetism in 2D CrI_3 by electrostatic doping. *Nat. Nanotechnol.* **2018**, *13*, 549–553. [CrossRef]
18. Klein, D.R.; MacNeill, D.; Lado, J.L.; Soriano, D.; Navarro-Moratalla, E.; Watanabe, K.; Taniguchi, T.; Manni, S.; Canfield, P.; Fernandez-Rossier, J.; et al. Probing magnetism in 2D van der Waals crystalline insulators via electron tunneling. *Science* **2018**, *360*, 1218–1222. [CrossRef]
19. Gibertini, M.; Koperski, M.; Morpurgo, A.F.; Novoselov, K.S. Magnetic 2D materials and heterostructures. *Nat. Nanotechnol.* **2019**, *14*, 408–419. [CrossRef]
20. Zhuo, W.; Lei, B.; Wu, S.; Yu, F.; Zhu, C.; Cui, J.; Sun, Z.; Ma, D.; Shi, M.; Wang, H.; et al. Manipulating Ferromagnetism in Few-Layered $Cr_2Ge_2Te_6$. *Adv. Mater.* **2021**, *33*, 2008586. [CrossRef]
21. Liu, W.; Guo, X.; Schwartz, J.; Xie, H.; Dhale, N.U.; Sung, S.H.; Kondusamy, A.L.N.; Wang, X.; Zhao, H.; Berman, D.; et al. A Three-Stage Magnetic Phase Transition Revealed in Ultrahigh-Quality van der Waals Bulk Magnet CrSBr. *ACS Nano* **2022**, *16*, 15917–15926. [CrossRef] [PubMed]
22. Deng, Y.; Yu, Y.; Song, Y.; Zhang, J.; Wang, N.Z.; Sun, Z.; Yi, Y.; Wu, Y.Z.; Wu, S.; Zhu, J.; et al. Gate-tunable room-temperature ferromagnetism in two-dimensional Fe_3GeTe_2. *Nature* **2018**, *563*, 94–99. [CrossRef] [PubMed]

23. Liu, Y.; Stavitski, E.; Attenkofer, K.; Petrovic, C. Anomalous Hall effect in the van der Waals bonded ferromagnet Fe_3-x$GeTe_2$. *Phys. Rev. B* **2018**, *97*, 165415. [CrossRef]
24. Chen, G.; Zhang, Y.; Qi, S.; Chen, J.-H. Gate-controlled magnetic transitions in Fe_3GeTe_2 with lithium ion conducting glass substrate. *Chin. Phys. B* **2021**, *30*, 097504. [CrossRef]
25. Huang, Y.; Wu, J.; Xu, X.; Ho, Y.; Ni, G.; Zou, Q.; Koon, G.K.W.; Zhao, W.; Castro Neto, A.H.; Eda, G.; et al. An innovative way of etching MoS_2: Characterization and mechanistic investigation. *Nano Res.* **2013**, *6*, 200–207. [CrossRef]
26. Wang, Z.; Li, Q.; Xu, H.; Dahl-Petersen, C.; Yang, Q.; Cheng, D.; Cao, D.; Besenbacher, F.; Lauritsen, J.V.; Helveg, S.; et al. Controllable etching of MoS_2 basal planes for enhanced hydrogen evolution through the formation of active edge sites. *Nano Energy* **2018**, *49*, 634–643. [CrossRef]
27. Tang, Q.-Y.; Yang, M.-J.; Yang, S.-Y.; Xu, Y.-H. Enhanced photocatalytic degradation of glyphosate over 2D CoS/BiOBr heterojunctions under visible light irradiation. *J. Hazard. Mater.* **2021**, *407*, 124798. [CrossRef]
28. Yang, L.; Majumdar, K.; Liu, H.; Du, Y.; Wu, H.; Hatzistergos, M.; Hung, P.Y.; Tieckelmann, R.; Tsai, W.; Hobbs, C.; et al. Chloride Molecular Doping Technique on 2D Materials: WS_2 and MoS_2. *Nano Lett.* **2014**, *14*, 6275–6280. [CrossRef]
29. Chao-Yi Cai, J.-H.C. Electronic transport properties of Co cluster-decorated graphene. *Chin. Phys. B* **2018**, *27*, 67304. [CrossRef]
30. Cao, S.; Cao, C.; Tian, S.; Chen, J.-H. Evidence of tunable magnetic coupling in hydrogenated graphene. *Phys. Rev. B* **2020**, *102*, 045402. [CrossRef]
31. Chen, J.H.; Jang, C.; Adam, S.; Fuhrer, M.S.; Williams, E.D.; Ishigami, M. Charged-impurity scattering in graphene. *Nat. Phys.* **2008**, *4*, 377–381. [CrossRef]
32. Chen, J.-H.; Cullen, W.G.; Jang, C.; Fuhrer, M.S.; Williams, E.D. Defect Scattering in Graphene. *Phys. Rev. Lett.* **2009**, *102*, 236805. [CrossRef]
33. Ohno, H.; Munekata, H.; Penney, T.; von Molnár, S.; Chang, L.L. Magnetotransport properties of p-type (In, Mn) As diluted magnetic III-V semiconductors. *Phys. Rev. Lett.* **1992**, *68*, 2664–2667. [CrossRef]
34. Tian, C.-K.; Wang, C.; Ji, W.; Wang, J.-C.; Xia, T.-L.; Wang, L.; Liu, J.-J.; Zhang, H.-X.; Cheng, P. Domain wall pinning and hard magnetic phase in Co-doped bulk single crystalline Fe_3GeTe_2. *Phys. Rev. B* **2019**, *99*, 184428. [CrossRef]
35. O'Hara, D.J.; Brubaker, Z.E.; Stillwell, R.L.; O'Bannon, E.F.; Baker, A.A.; Weber, D.; Aji, L.B.B.; Goldberger, J.E.; Kawakami, R.K.; Zieve, R.J.; et al. Suppression of magnetic ordering in Fe-deficient $Fe_{3-x}GeTe_2$ from application of pressure. *Phys. Rev. B* **2020**, *102*, 054405. [CrossRef]
36. Drachuck, G.; Salman, Z.; Masters, M.W.; Taufour, V.; Lamichhane, T.N.; Lin, Q.; Straszheim, W.E.; Bud'ko, S.L.; Canfield, P.C. Effect of nickel substitution on magnetism in the layered van der Waals ferromagnet Fe_3GeTe_2. *Phys. Rev. B* **2018**, *98*, 144434. [CrossRef]
37. Chowdhury, R.R.; DuttaGupta, S.; Patra, C.; Tretiakov, O.A.; Sharma, S.; Fukami, S.; Ohno, H.; Singh, R.P. Unconventional Hall effect and its variation with Co-doping in van der Waals Fe_3GeTe_2. *Sci. Rep.* **2021**, *11*, 14121. [CrossRef]
38. May, A.F.; Calder, S.; Cantoni, C.; Cao, H.; McGuire, M.A. Magnetic structure and phase stability of the van der Waals bonded ferromagnet $Fe_{3-x}GeTe_2$. *Phys. Rev. B* **2016**, *93*, 014411. [CrossRef]
39. Tian, Y.; Ye, L.; Jin, X. Proper Scaling of the Anomalous Hall Effect. *Phys. Rev. Lett.* **2009**, *103*, 087206. [CrossRef]
40. Nagaosa, N.; Sinova, J.; Onoda, S.; MacDonald, A.H.; Ong, N.P. Anomalous Hall effect. *Rev. Mod. Phys.* **2010**, *82*, 1539–1592. [CrossRef]
41. Saha, P.; Singh, M.; Nagpal, V.; Das, P.; Patnaik, S. Scaling analysis of anomalous Hall resistivity and magnetoresistance in the quasi-two-dimensional ferromagnet Fe_3GeTe_2. *Phys. Rev. B* **2023**, *107*, 035115. [CrossRef]
42. Tan, C.; Lee, J.; Jung, S.-G.; Park, T.; Albarakati, S.; Partridge, J.; Field, M.R.; McCulloch, D.G.; Wang, L.; Lee, C. Hard magnetic properties in nanoflake van der Waals Fe_3GeTe_2. *Nat. Commun.* **2018**, *9*, 1554. [CrossRef] [PubMed]